J. Fluid Mech. (1970), *vol.* 41, *part* 1, *pp.* 13–46
Boeing Symposium on Turbulence

Entrainment and the structure of turbulent flow

By A. A. TOWNSEND
Emmanuel College, Cambridge

(Received 4 August 1969)

Although the entrainment of non-turbulent fluid into a turbulent flow occurs across sharply defined boundaries, its rate is not determined solely by the turbulent motion adjacent to the interface but depends on overall properties of the flow, in particular, on those that control the energy balance. In the first place, attention is directed to the many observations which show that the motion in many turbulent shear flows has a structure closely resembling that produced by a rapid, finite, plane shearing of initially isotropic turbulence. The basic reasons for the similarity are the stability and permanence of turbulent eddies and the finite distortions undergone by fluid parcels in free turbulent flows. Next, the existence of eddy similarity and the condition of overall balance of energy are used to account for the variation of entrainment rates within groups of broadly similar flows, in particular mixing layers between streams of different velocities and wall jets on curved surfaces. For some flows which satisfy the ordinary conditions for self-preserving development, no entrainment rate is consistent with the energy balance and self-preserving development is not possible. Examples are the axisymmetric, small-deficit wake and the distorted wake. Finally, the implications of an entrainment rate controlled by the general motion are discussed. It is concluded that the relatively rapid entrainment in a plane wake depends on an active instability of the interface, not present in a constant-pressure boundary layer whose slow rate of entrainment is from 'passive' distortion of the bounding surface by eddies of the main turbulent motion. Available observations tend to support this conclusion.

1. Introduction

Most free turbulent flows depend for their energy supply on converting mean-flow energy to turbulent energy by entrainment of non-turbulent ambient fluid, and it is natural to see in the actual processes of entrainment the key to the mean-flow problem of turbulence, the prediction of mean velocities and turbulent stresses. In fact, the entrainment process is only one of a group of processes whose combined interactions determine the level of turbulent energy dissipation and the entrainment rate, and it is not immediately clear that any one of them is the dominant influence. In some respects, an analogy may be drawn with the closed control-loops of servo-mechanisms and feed-back circuits where all elements of the loop are essential for its operation but the important properties are controlled by one particular element and are nearly independent of the remainder. At a

Printed in Great Britain

time when much attention is being paid to the form and motion of the bounding surface over which the entrainment occurs, it is desirable to emphasize that details of the entrainment process will be dynamically similar in different flows—in jets, wakes and boundary layers—only if the entrainment mechanism is the dominant element of the 'control loop'. If it is not, the rate of entrainment and perhaps the nature of the entrainment process will be affected by other elements.

Another important element of the 'control loop' is the production and dissipation of turbulent energy deep within the flow and, long before the discovery of the sharply defined boundary between turbulent and non-turbulent fluid, the mixing-length theories of L. Prandtl and of G. I. Taylor used, in effect, the energy balance and an assumption of structural similarity of turbulent motion. More recently, Bradshaw, Ferriss & Atwell (1967) have refined this approach and have been able to predict the development of boundary layers in a wide variety of pressure gradients. The interesting point about their work is that it determines an entrainment rate in good agreement with observation while completely ignoring details of the entrainment mechanism. My purpose here is to discuss the nature and origin of the 'universal' structure of fully sheared turbulence as it appears in different flows, to give examples of the prediction of entrainment rates, and to suggest how the entrainment mechanism conforms to the wide range of entrainment rates prescribed by the structural similarity and the energy balance.

2. Notation and axes of reference

With stated exceptions, two-dimensional mean flows are considered, homogeneous in the $0y$ direction, with the general direction of flow in the $0x$ direction and with the strongest gradients of mean values in the $0z$ direction. For convenience, the subscript notation is also used so that a position vector may have components (x, y, z) or (x_1, x_2, x_3). Then:

U, 0, W are the components of the mean velocity;

u, v, w are the components of the velocity fluctuation, $q^2 = u^2 + v^2 + w^2$;

P is the mean pressure;

U_1, 0, W_1 are the components of the mean velocity outside the turbulent flow;

$R_{ij}(\mathbf{r}; \mathbf{x}) = \overline{u_i(\mathbf{x})\, u_j(\mathbf{x}+\mathbf{r})}$ is the double velocity correlation function;

$\tau = -\overline{uw}$ is the turbulent Reynolds stress; *or* τ is the time-interval for space-time correlations;

L is the integral scale of the hypothetical, initially isotropic turbulence before distortion;

α is the total or effective strain at a point;

ν_t is the eddy viscosity;

D_t is the eddy diffusivity for effective strain;

u_0, q_0 are the scales of mean velocity variation and of velocity fluctuation for a section of the flow;

l_0 is a length scale for the section;

β is a non-dimensional entrainment constant (not yet defined);

$R_s = u_0 l_0 / \nu_T$ is a flow constant, defined so that u_0 is the maximum difference of

mean velocity across the flow, l_0 is the variance of the velocity distribution about its maximum value (or, for mixing layers, the variance of the velocity gradient), and ν_T is the average eddy viscosity obtained by fitting the calculated profile for constant eddy viscosity to the measured mean velocity profile. Note that β and R_s are independent of position in any one self-preserving flow but take different values in different flows.

3. The behaviour of eddy structures in homogeneous turbulence

A remarkable feature of turbulent flows is the comparative stability and permanence of the flow patterns that are usually called eddies. Use of the term eddy implies that the whole motion can be considered to be composed of the superposition of the velocity fields of many simple elementary eddies, not much more complex in structure than the Hill spherical vortex or the vortex ring. For the concept to be useful, the duration of a single eddy must be relatively long and measurements in homogeneous turbulence show that the degree of permanence is remarkable.

A good example is the slowness with which grid turbulence approaches the statistically most probable state of isotropy. Comte-Bellot & Corrsin (1966) find that the index of anisotropy, $\overline{u_1^2}/\overline{u_2^2} - 1$, decreases by a factor of two while the energy decreases by a factor of twenty. The implication that the eddies lose energy and decay without considerable change in their flow patterns is confirmed in more detail by measurements of space-time correlations by Favre, Gaviglio & Dumas (1962, p. 419) and by Frenkiel & Klebanoff (1967). The correlations trace the changes in velocity pattern in a frame moving with the mean flow, which may be caused either by bodily translation of whole eddies in the velocity fields of their neighbours, by a self-induced velocity of propagation like that of a vortex-ring, or by real changes in the velocity patterns of individual eddies. Bodily translations 'diffuse' the correlation function while changes of pattern reduce its magnitude, and the contributions of translation and pattern change can be calculated from the observations (appendix A). From the measurements of Favre *et al.* for a non-dimensional time delay, $U_1\tau/M = 7{\cdot}57$, it is estimated that the auto-correlation coefficient for individual eddies is 0·85, compared with a correlation coefficient moving with the mean flow of 0·41 and an energy reduction in the ratio 0·80. It is probable that some of the loss of auto-correlation is an effect of the increase in diameter of typical eddies by the diffusive action of small eddies, the increase being about 10% over the time interval. In any event, the larger energy-containing eddies of grid turbulence retain their basic structure over periods long enough for a large part of their energy to be dissipated by turbulent transfer to smaller eddies.

If the larger eddies in shear-free turbulent flow are very stable structures, it appears likely that mean velocity gradients only distort the velocity patterns without causing their disintegration. In terms of the Fourier representation of the velocity field, stability of large eddies during substantial decay means that the non-linear transfer of energy from components of small wave-number (the larger eddies) to those of considerably larger wave-number is qualitatively similar

in action to an effective viscosity and that transfer between components of comparable wave-numbers is weak. Then the effect of a mean velocity gradient is to modify and to redistribute the energy of components forming the larger eddies nearly in the way predicted by the rapid-distortion theory of Batchelor & Proudman (1954) or, better, by the modified form which models the transfer to smaller eddies by a coefficient of eddy viscosity (Pearson 1959).

If grid turbulence is passed through a duct of changing section, it is subjected to homogeneous, irrotational distortion and many observations of its behaviour have been made, particularly for plane straining. The most extensive are those by Tucker & Reynolds (1968) and by Maréchal (1967) and they show that (i) the ratios of the intensities of the turbulence component velocities continue to change with increasing strain and show no sign that an equilibrium structure develops after long straining, and (ii) if some allowance is made for contributions from the less anisotropic smaller eddies, the ratios are not dissimilar from those predicted by the rapid-distortion theory. Available measurements of correlation and spectrum functions are in good agreement with predictions from the theory (see figure 1 and Townsend (1954)).

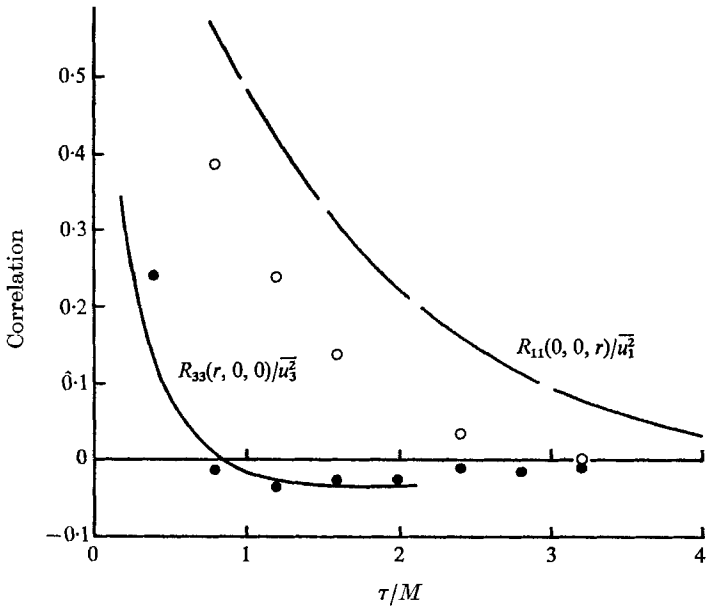

FIGURE 1. Comparison of calculated correlations for irrotational plane shear with measurements by Grant (1958). ($0x_1$ is the direction of expansion, $0x_3$ is the direction of compression, and the calculated correlations are for a total strain ratio of four. The 'initial' integral scale is taken as $L = \frac{1}{2}M$.)

In ordinary shear flows the distortion by the mean flow is nearly a plane shearing with rotation, and it is not possible to produce such a distortion by changes in the duct section. Rose (1966) has measured turbulence in the flow behind a non-uniform grid designed to produce a uniform gradient of velocity transverse to the stream, and he found that the intensities of the three components appear

to approach asymptotic values for total strains greater than two. Comparison with the theory is made uncertain by lack of knowledge of the initial motion just downstream of the grid, but the results are in very fair agreement with those calculated assuming rapid distortion and plausible values for the transfer to smaller eddies (for details see appendix B). Predicted variations of the intensities are shown in figures 2 and 3, and it is seen that, although no asymptotic universal structure is expected, the intensity ratios vary little for total strains in the range 1·5–3·5. Since the maximum strain in the experiments was less than three, experiment and theory agree on this point. Lastly, those components of the correlation function that were measured agree well with the predicted forms (figure 4).

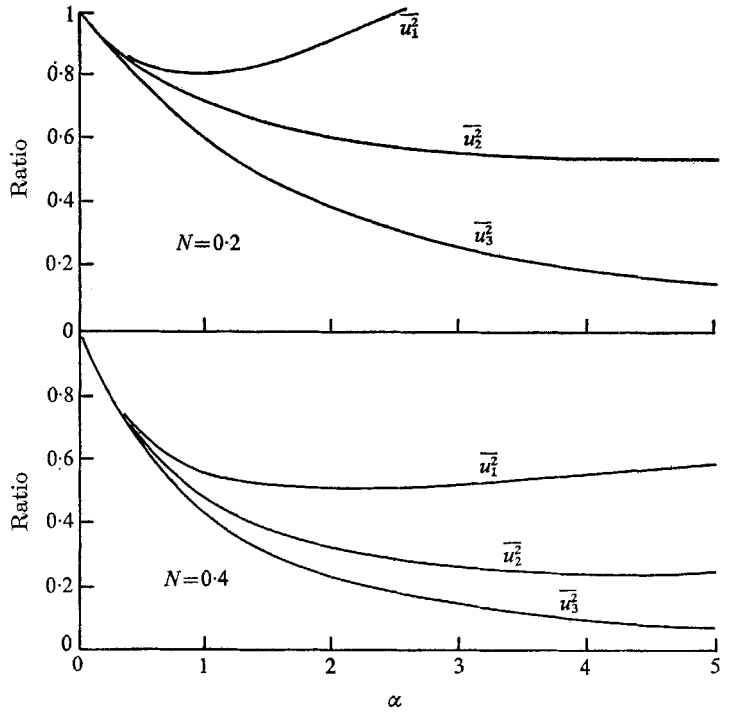

FIGURE 2. Variation with total shear of intensities of the velocity components, calculated from the rapid-distortion approximation for two values of N.

4. The structure of turbulence in shear flows

Since free turbulent flows continually entrain ambient fluid, the 'ages' of parcels of turbulent fluid, i.e. the times that have elapsed since they were first entrained and became turbulent, are usually comparable with local time-scales at their present position, among others the reciprocal of the local velocity gradient. Then the total strain experienced by any parcel is not large compared with one and it is probable that the structure of the existing turbulence is the product of finite distortion of turbulent motion generated by the entrainment process. Whether the actual entrainment process is a runaway instability of the

the bounding surface, overturning by the main eddies of the turbulence, or a 'nibbling' by the smallest eddies, the resultant initial motion is likely to be quasi-isotropic in the sense that it is not highly organized and spatially orientated. To test the hypothesis, measurements of correlation functions in ordinary shear flows can be compared with the predictions of the rapid-distortion theory for a moderate total strain. Intensities and correlation functions have been calculated for initially isotropic turbulence with the 'exponential' correlation function,

$$R_{ij}(\mathbf{r}) = u_0^2\left[\delta_{ij}(1-\tfrac{1}{2}r/L)+\frac{1}{2}\frac{r_i r_j}{rL}\right]e^{-r/L}, \tag{4.1}$$

that has undergone plane shearing with a total strain ratio of two. The actual value of the ratio does not seem to be critical.

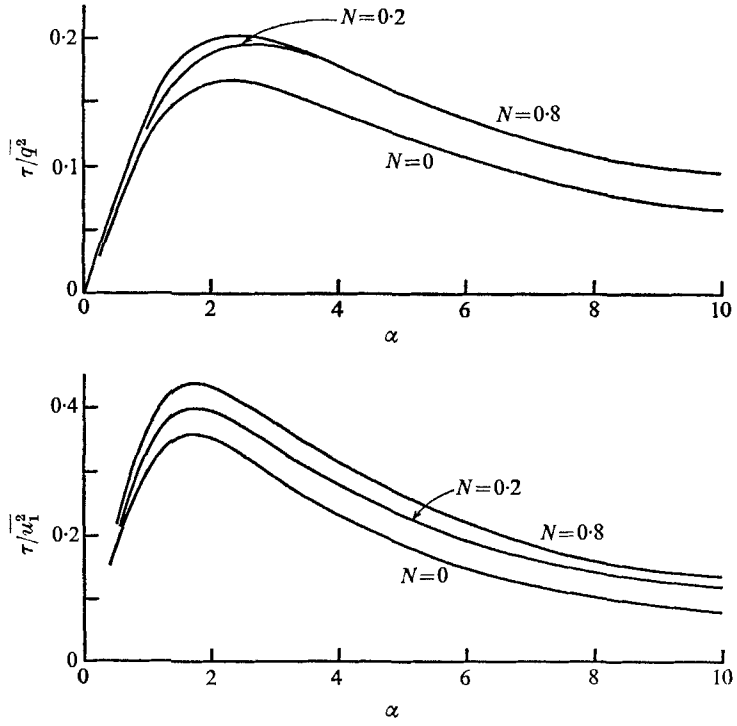

FIGURE 3. Variation with total shear of ratios of Reynolds stress to turbulent intensities, calculated from the rapid-distortion theory for three values of N.

From figure 5 it can be seen that the set of 'normal' correlation functions—those with displacements parallel to the axes of reference—has a surprisingly complex structure, suggesting that the distortion selects eddy structures of a highly characteristic form. The contours of equal correlation in the $x_1 0 x_3$ plane (figure 6) are also not simple, being nearly symmetrical about the axes for R_{33} and R_{13} and elongated at an angle to the axes for R_{11} and R_{22}. Because of the complexity, a close resemblance between the calculated correlations and observations in real shear flows must be regarded as a strong indication that the eddies

in real shear flows are selected from unorganized turbulence by the shearing in the manner described by the rapid-distortion theory.

The measurements of Grant (1958) are still possibly the most comprehensive and, in figure 7, his measurements of the normal correlation functions in a turbulent wake are compared with the calculated ones. For the set of nine curves, the only disposable constants are a single length scale and the total strain. Many other, less comprehensive, measurements in other flows have been made, and table 1 compares the observed and predicted forms of the normal correlations, using a simple code to specify the general form of the correlation curve, i.e. whether or not it takes negative values, and its scale. Except for measurements in the cylindrical mixing layer of a circular jet where vortex rings are the dominant elements of the flow, the agreement is very good.

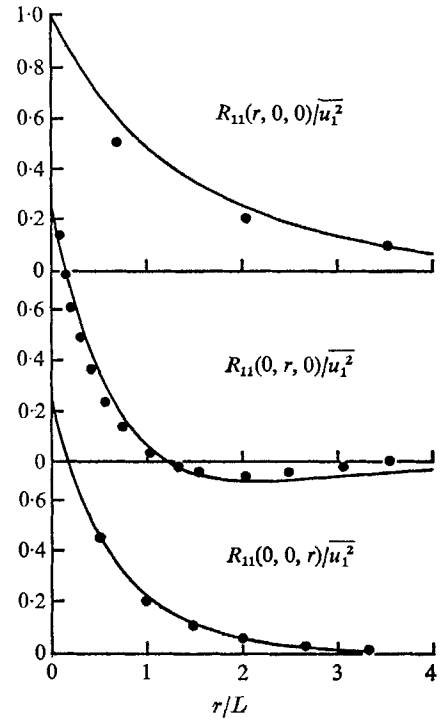

FIGURE 4. Comparison of calculated correlations with the measurements of Rose (1966). (At $Y/h = 0{\cdot}5$, $X/h = 9{\cdot}0$, except for $R_{11}(r, 0, 0)$ for which $X/h = 7{\cdot}5$. The 'initial' integral scale is taken to be 1·0 in.)

Measurements of correlations with displacements inclined to the usual axes are less common, the most extensive being those of Grant in the wake and the boundary layer and of Tritton (1967) in the boundary layer. The shape of the correlation contours for displacements in the $x_1 0 x_3$ plane determines whether correlation curves for constant lateral (r_3) displacement have their maximum value at zero streamwise displacement or not. Asymmetry of the $R_{11}(r_1, 0, r_3)$ correlation was first reported by Favre, Gaviglio & Dumas (1957) in their measurements of space-time correlations in a boundary layer, and later measurements of

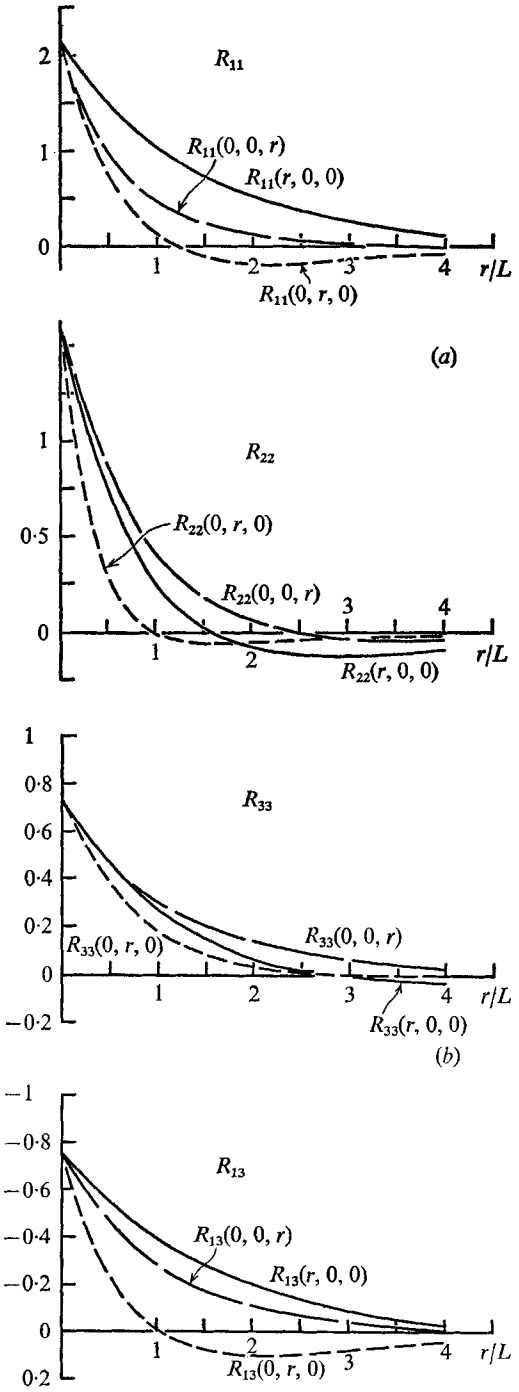

FIGURE 5. Normal components of the correlation function calculated for $\alpha = 2$.

Component	Rapid distortion		Homogeneous shear		Wake		Cylindrical mixing layer		Inner boundary layer		Outer boundary layer		Channel	
	+	−	+	−	+	−	+	−	+	−	+	−	+	−
R_{11} $(r, 0, 0)$	4·2	—	5·1	—	6	—		8 (0·05)	30	—	5	—	5	—
R_{11} $(0, r, 0)$	—	1·2 (0·08)	—	1·2 (0·06)	—	2·3 (0·08)	—	4·2 (0·15)	—	2·6 (0·02)	—	1·7 (0·12)	—	1·4 (0·13)
R_{11} $(0, 0, r)$	—	3·5 (0·01)	2·1	—	5	—		?	7	—	—	2·9 (0·03)	2·2	—
or	2·2	—												
R_{22} $(r, 0, 0)$	—	1·6 (0·10)		?	—	2·3 (0·08)	—	4 (0·18)	7	—	—	2·2 (0·08)		?
R_{22} $(0, r, 0)$	—	2·5 (0·035)		?	—	3·1 (0·06)	9	—	—	5 (0·02)	3·0	—	1·5	—
R_{22} $(0, 0, r)$	—	1·0 (0·045)		?	—	1·8 (0·03)		?	—	1·3 (0·06)	—	1·3 (0·06)	—	1·2 (0·08)
R_{33} $(r, 0, 0)$	—	2·9 (0·04)		?	—	1·5 (0·16)	—	4 (0·14)	4·4	—	—	1·9 (0·06)		?
R_{33} $(0, r, 0)$	—	3·5 (0·002)		?	4	—	—	6 (0·02)	1·4	—	—	2 (0·02)	—	1·0 (0·02)
or	1·9	—												
R_{33} $(0, 0, r)$	3·8	—		?	3·5	—		—	7	—	4	—	3	—
R_{13} $(r, 0, 0)$	3·8	—		?		?		?		?	4	—		?
R_{13} $(0, r, 0)$	—	1·05 (0·12)		?		?		?	—	3 (0·20)	—	0·8 (0·18)		?
R_{13} $(0, 0, r)$	3·2	—	3·1	—		?		?		?	3	—		?

TABLE 1. Normal correlation functions in shear flows

Notes. An entry in the '+' column indicates that the correlation does not change sign, and the number is the value of r for which the correlation is 0·05 of its maximum value. An entry in the '−' column indicates that the correlation changes sign, the number outside the bracket gives the value of r at cross-over, and the one inside the bracket gives the maximum of reversed sign as a fraction of the value for $r = 0$. The calculated, rapid-distortion, entries are given in both forms if the correlations of reversed sign are less than 0·01 of the maximum. For each flow the scale of length has been chosen to make comparison convenient but preserving the ratios of scales in each flow. No information is denoted by '?'.

Sources are: Homogeneous shear—Rose (1966); wake, inner and outer boundary layer—Grant (1958); cylindrical mixing layer—Bradshaw *et al.* (1964); two-dimensional channel—Comte-Bellot (1961).

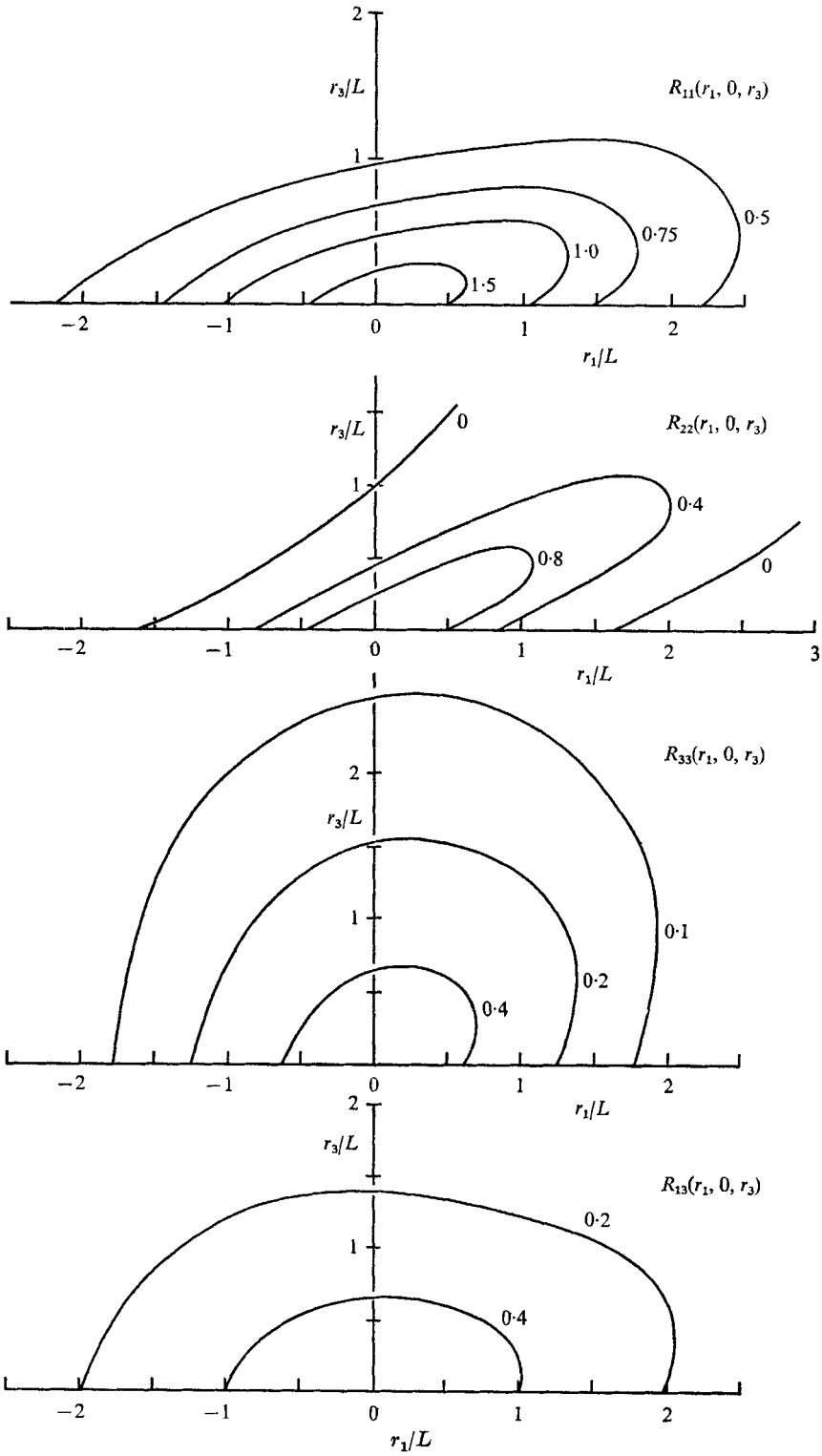

FIGURE 6. Contours of constant correlation in the plane $r_2 = 0$, calculated for $\alpha = 2$.

this and other correlations agree with the predictions (table 2). Excepting the measurements in the cylindrical mixing layer, differences between the observed and predicted forms of the correlation function are very few and may plausibly be attributed either to small experimental errors or to the influence of entraining motions that are not properly part of the main turbulent structure.

Flow	R_{11}	R_{22}	R_{33}	R_{13}
Rapid distortion	1·5	1·5	0·3	0
Wake (Grant 1958)	1·2	1·2	0·1	?
Boundary layer				
(Favre *et al.* 1957)	3	?	?	?
(Grant 1958)	?	?	0·2	?
(Tritton 1967)	1·5	?	0	0·7
(Bowden & Howe 1963)	1·5	?	0	?

Notes. The tabulated values are of r_m/r_3 where r_m is the value of r_1 for which $R_{ij}(r_1, 0, r_3)$ has a maximum value of about 0·5 with respect to variation of r_1, i.e.

$$\frac{\partial R_{ij}}{\partial r_1} = 0 \quad \text{and} \quad R_{ij} = 0{\cdot}5.$$

The direction of the $0x_1$ axis is always chosen so that $\partial U_1/\partial x_3$ is positive.
No information is denoted by '?'.

TABLE 2. Positions of maximum correlations for separations with constant displacement in $0x_3$ direction

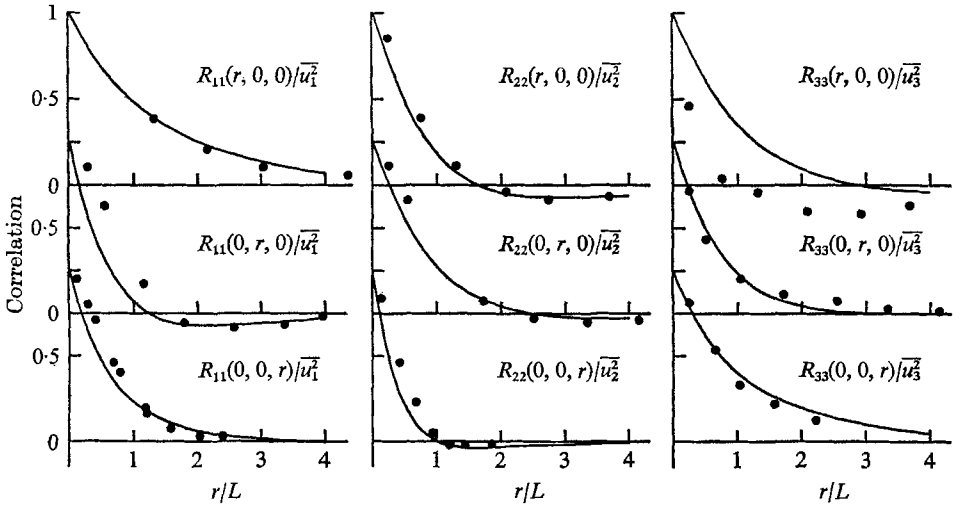

FIGURE 7. Comparison of calculated normal components of the correlation function with the measurements of Grant (1958) in a plane wake. ($U_1 d/\nu = 1300$, $x/d = 533$, fixed wire at $z/d = 4$ except for $R_{33}(0, 0, r)$ for which $z/d = 2{\cdot}8$. The 'initial' integral scale is taken as $L = 3d$ and the total strain is $\alpha = 2$.)

5. Effective total shear for free turbulent flow

With the evidence that the observed structure of the turbulent motion in shear flows resembles closely the motion arising from rapid, finite shear of isotropic turbulence, it is important to have an estimate of the magnitudes of

the total shear undergone by fluid parcels since their original entrainment into the turbulent flow. Supposing for the moment that the scale of the motion is small compared with the width of the flow, the total strain of a parcel is the time integral of the rate-of-strain along its path since entrainment, but different parcels successively at the same place will have travelled along different paths and have different total strains. Qualitatively, the variations of path affect the mean total strain in much the same way as an eddy diffusivity of the mean total or the effective strain, α. Since $\partial U/\partial z$ is the mean rate of strain, the effective strain satisfies the equation,

$$\frac{D\alpha}{Dt} = U\frac{\partial\alpha}{\partial x} + W\frac{\partial\alpha}{\partial z} = \frac{\partial U}{\partial z} + \frac{\partial}{\partial z}\left(D_T\frac{\partial\alpha}{\partial z}\right), \tag{5.1}$$

where D_T is the eddy diffusivity for effective strain.

It is not difficult to show that the equation for effective strain takes a self-preserving form if the flow is self-preserving. In a self-preserving flow for which

$$\left.\begin{aligned} U &= U_1 + u_0 f(z/l_0), \\ \alpha &= k(z/l_0), \end{aligned}\right\} \tag{5.2}$$

the equations for momentum and strain are

$$U_1\left(\frac{du_0}{dx}f - \frac{u_0}{l_0}\frac{dl_0}{dx}\eta f'\right) + u_0\frac{du_0}{dx}f^2 - \frac{u_0}{l_0}\frac{d(u_0l_0)}{dx}f'\int_0 f\,d\eta = \frac{\nu_T}{l_0^2}f'' \tag{5.3}$$

and

$$-U_1\frac{u_0}{l_0}\frac{dl_0}{dx}\eta k' - \frac{1}{l_0}\frac{d(u_0l_0)}{dx}k'\int_0 f\,d\eta = \frac{u_0}{l_0}f' + \frac{D_T}{l_0^2}k'', \tag{5.4}$$

assuming constant values across any section for the eddy viscosity ν_T and the diffusivity D_T. Appendix C deals with solutions of these equations, in particular for the case of equal eddy viscosity and diffusivity, with the results given in table 3.

Flow	Effective strain	Flow constant R_s
Wake	2·6	12·5
Jet	6·1	28
Mixing layer	7·5	30
Boundary layer (constant-pressure)	10–15	55

TABLE 3

A conclusion from the tabulated results is that the effective strain has a maximum value of about one-fifth of the flow constant $R_s = u_0l_0/\nu_T$, defined so that u_0 is the maximum variation of mean velocity across the flow and l_0 is the variance of the velocity distribution (for wakes and jets) or of the distribution of velocity gradient (for mixing layers and boundary layers). In similar flows, the proportionality of R_s and α_m is a consequence of the similarity of the distributions. At the position of maximum effective strain, the equation (5.1) reduces to

$$0 = \frac{\partial U}{\partial z} + D_T\frac{\partial^2\alpha}{\partial z^2} \tag{5.5}$$

and, assuming universal distributions of $(U-U_1)$ and of α, it follows that

$$\alpha_m = \frac{u_0 l_0}{D_T}\left[l_0^2\frac{\partial^2\alpha}{\partial z^2}\Big/\left(\frac{l_0}{u_0}\frac{\partial U}{\partial z}\right)\right]_{\alpha=\alpha_m} \tag{5.6}$$

With the ratio D_T/ν_T near one, maximum effective strain and maximum velocity gradient both occur near $z = l_0$, and near proportionality of α_m and R_s is to be expected.

The calculations of the maximum effective strains in free turbulent flows shows first that these strains are not large but also that there is considerable variation between one flow and another. Reasonable modifications of the basic assumptions are not likely to change these conclusions and, in view of the close resemblance between the spatial structures of shear turbulence and the 'rapid-distortion turbulence', it is profitable to compare intensity ratios observed in the various flows with the calculated ratios for total strains of the appropriate magnitudes. From figure 3, the predicted values of the ratio of the Reynolds stress to the total turbulent intensity, $\overline{q^2}$, are seen to reach a maximum value for total strain of about 2·5 and to decrease slowly for increase of strain, a result that is nearly unaffected by inclusion of a viscosity term to model the energy transfer to smaller eddies. The trend of total strains in table 3 suggests that the ratio should decrease systematically over the sequence—wakes, jets and mixing layers, boundary layers—and the rather erratic measurements tend to confirm the suggestion. The standing of the hypothesis of structural similarity is: (i) that eddies of complex but broadly similar structure are the dominant eddies in all shear flows; (ii) that the stress-intensity ratio, τ_m/q_0^2, is roughly the same in all flows, simply because the effective strains are not far from the value for maximum of the ratio, $\tau/\overline{q^2}$; and (iii) that the variation of the stress-intensity ratio between different flows is not negligible and has a systematic dependence on the effective strain, in its turn dependent on the flow constant, R_s.

6. The dominant eddies in inhomogeneous shear flow

All real shear flows are more or less strongly inhomogeneous and the appearance in them of eddies that are very similar to those found in homogeneous shear flows needs some explanation. Any explanation must involve the form of the dominant eddies of the flow, and there are two ways of arriving at the form from the correlation functions. The most objective is that of Lumley (1965, p. 166) which involves considerable computation. The alternative is a mixture of inference and guesswork based on the form of the correlation functions and, for a two-dimensional wake, Payne (1966), using the Lumley method, and Grant (1958), guessing, have arrived at fairly similar conclusions. A simple model that accounts for most of the features of the calculated correlations is sketched in figure 8. The eddy streamlines (relative to the mean flow) lie nearly on the surfaces of two cylinders with parallel axes inclined in the $x_1 0 x_3$ plane and separated in the $0x_2$ direction, and their planes of circulation have normals more inclined to the $0x_1$ direction than the axes of the cylinders. Certain features of the correlation make it clear that regions of 'negative Reynolds stress', i.e. positive uw

product, are present and so the circulation cannot be exactly in a plane. The flow pattern will be called a double-roller eddy, but it might also be described as a section of a linear jet or as a diffused vortex-pair. It resembles closely the eddies studied in boundary-layer and pipe flow by Kline *et al.* (1967).

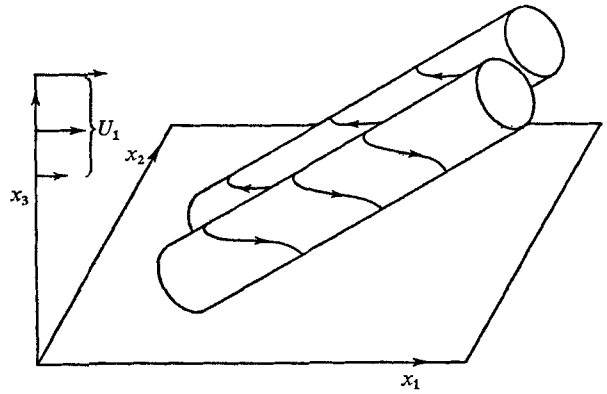

FIGURE 8. Sketch of inclined double-roller eddy. (Arrows on the lines around the cylinder indicate the streamlines of the eddy.)

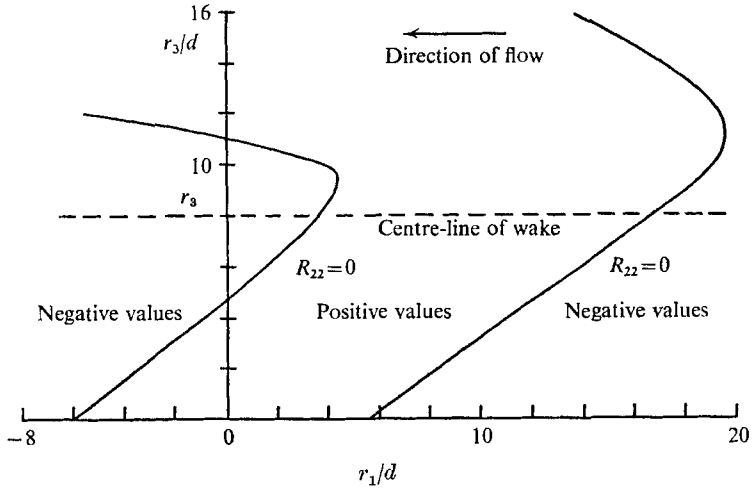

FIGURE 9. Contours of zero $R_{22}(r_1, 0, r_3)$ measured in a plane wake by Grant (1958). To simplify comparison with the contours in figure 6, which refer to positive rate-of-strain, the co-ordinates have been changed so that the fixed wire is at $x_3/d = -7{\cdot}6$ and the direction of r_1 is opposite to the direction of flow.

In inhomogeneous flows such as a wake, the sense of the velocity gradients changes across the central plane of symmetry and it is found that the roller axes reverse their inclination to the $0x_1$ direction so that each roller of the eddy is deformed into a bent, hair-pin shape. The effect is well shown by Grant's measurements of the $R_{22}(r_1, 0, r_3)$ correlation (which is little affected by the motions responsible for entrainment), shown in figure 9, and it appears both in

his reconstruction of the eddies and in that of Payne. It appears that each *section* of the double-roller interacts with the mean volocity gradient in much the same way as if it were in a homogeneous field, and that the coherence of motion between different sections is limited to general alignment and matching of circulation in the $x_1 0 x_2$ plane. The behaviour may be connected with the comparatively compact form of the eddy in the direction of shear.

To use the concept of structural similarity in the description of the mean flow properties, two assumptions must be made. The first is that the ratio of Reynolds stress to total intensity is either constant or a known function of the effective strain. The second concerns the dissipation length-parameter, i.e. the effective length scale of the dominant eddies for transfer of energy from them to the smaller eddies. There is good experimental evidence that it is nearly the same fraction of the flow width in a variety of flows, possibly because the dominant eddies are as large as they can be within the turbulent fluid.

7. Entrainment constants of self-preserving flows

By assuming similarity of the profiles and mean velocity, turbulent intensity and rate of energy dissipation, it is possible to give a unified description of the rates of spread of all self-preserving jets and wakes (Townsend 1966; Newman 1968). The basic assumptions are that in all the flows, the profiles have the forms,

$$\left.\begin{aligned} U - U_1 &= u_0 f(z/l_0), \\ \overline{q^2} &= q_0^2 g(z/l_0), \\ \epsilon &= q_0^3/l_0 h(z/l_0), \end{aligned}\right\} \tag{7.1}$$

where f, g, h are universal functions, and u_0, q_0, l_0 are scales of velocity and length depending on x in the particular flow. By inserting these expressions in the equations for the overall balances of momentum and total energy,

$$\left.\begin{aligned} \int \frac{\partial}{\partial x}[U(U-U_1)]\,dz + \frac{dU_1}{dx}\int (U-U_1)\,dz &= -\tau_0, \\ \frac{1}{2}\int \frac{\partial}{\partial x}[U\{(U-U_1)^2+\overline{q^2}\}]\,dz + \frac{dU_1}{dx}\int (U-U_1)^2\,dz &= -\int \epsilon\,dz - \tau_0(U_0-U_1), \end{aligned}\right\} \tag{7.2}$$

it is possible to obtain an equation for the entrainment constant,

$$\beta = \frac{U_1 + \frac{1}{2}u_0}{u_0}\frac{dl_0}{dx}, \tag{7.3}$$

whose coefficients are non-dimensional integrals of the distribution functions and the ratio of the scale of turbulent velocities, q_0, to the scale of mean velocity variation, u_0. In any particular self-preserving flow, the ratio is constant but it varies from flow to flow.

From the momentum equation the ratio of maximum stress to u_0 can be calculated, and then the ratio q_0/u_0 can be found if the effective value of τ_m/q_0^2 is known. Defining the velocity scale of the turbulent motion so that q_0^2 is an average intensity for the whole flow, the stress-intensity ratio at the position of

maximum stress is a good approximation to the effective value of τ_m/q_0^2. The previous discussion of effective strain and the predictions of the rapid-distortion theory indicate that $\tau/\overline{q^2}$ is not constant but diminishes slowly as the effective strain, which is nearly proportional to the flow constant and inversely proportional to the entrainment constant, increases.

For strain ratios above four, a range covering jets, mixing layers and boundary layers but not wakes, the variation of $\tau/\overline{q^2}$ can be approximated by

$$\tau/\overline{q^2} \propto \alpha^{-n},$$

where n is less than one. For flows with similar distributions of velocity and shear stress,

$$\frac{\tau_m}{q_0^2} \propto R_s \propto \alpha,$$

and so $\tau_m^{\frac{1}{2}(n+1)} \propto u_0 q_0$. If $n = 1$, this agrees with the 'mixing-length' relation proposed by Newman (1968). The non-linear diffusion model of Nee & Kovasznay (1969) implies that R_s is a constant fraction of q_0^2/u_0^2, equivalent to $n = 0$ and $\tau_m/q_0^2 =$ constant or to similarity of the turbulent motion in all flows.

To illustrate the procedure for normal self-preserving flows, details are given in appendices D and E for plane mixing layers with different velocities of the bounding streams and for wall jets on curved surfaces. For the plane mixing layers, the analysis shows that the entrainment constant, in this case

$$\beta = \frac{U_1 + U_2}{U_1 - U_2} \frac{dl_0}{dx}, \tag{7.4}$$

is nearly independent of the velocity ratio U_2/U_1, in agreement with observations by Sabin (1963). The result is that expected from elementary dimensional arguments, but the case of the wall jets is more interesting. It is known that a curved wall jet spreads less rapidly on a convex surface than on a concave surface, and it is usual to explain the effect in terms of the inertial stability or instability of mean flow with curved streamlines. Although the structure and intensity of the turbulent motion may be affected directly by curvature of the mean flow, application of the similarity assumptions leads to a predicted dependence of angle of spread on curvature that is close to the observed values. Fekete (1963) finds that wall jets on cylinders have angles of spread given by (in the present notation)

$$dl_0/dx = C(1 + 3{\cdot}75 l_0/R), \tag{7.5}$$

while the similarity calculations give the coefficient of l_0/R as 4·8 if τ_m/q_0^2 is independent of effective strain (R is the radius of curvature of the surface, positive for a concave surface). If the stress-intensity ratio varies in the expected way, the coefficient is less but the observed effect of curvature remains not far from the value found assuming no change of structure. The effect of curvature involved depends on changes in the stress distribution needed to balance the effects of the lateral pressure distribution induced by the curvature of the flow.

The equations for the entrainment constants obtained from the similarity

assumption have the form,

$$(\text{shape parameters}) + \beta \frac{q_0^2}{\tau_m} (\text{shape parameters}) = \beta^{\frac{1}{2}} \left(\frac{q_0^2}{\tau_m} \right)^{\frac{3}{2}} (\text{shape parameters}), \tag{7.6}$$

the bracketed terms depending only on the shapes of the distributions of mean velocity and turbulent intensity. The first term represents the gain of mean flow energy by advection, the second the gain of turbulent energy by advection, and the third the loss of energy by turbulent dissipation. The first and third are always positive but the second is positive in jets and wakes but negative in mixing layers and in most boundary layers. If the turbulent advection term is positive, there may be no real positive solution for β, and no self-preserving development is possible although the ordinary conditions for self-preserving development (e.g. Townsend 1956) are satisfied. Three examples of this behaviour are known. The first is the periodic wake behind a grid of equally spaced, circular cylinders in which the mean velocity variation decreases exponentially with distance while the turbulent intensity varies inversely as distance (Stewart 1951). A second is the far wake of an axisymmetric body. Here Baldwin & Sandborn (1968) and Gibson, Lin & Chen (1967) have found intermittently turbulent flow over the whole flow, and Baldwin & Sandborn find that the intermittency factor on the centre-line increases with distance from the body. Schlieren photographs of projectile wakes do not show intermittency on the axis. A possible reason is that the schlieren picture shows the total fluctuations along a line of sight while the intermittency probably arises from the development of 'holes' in fully turbulent fluid by a process of 'reverse transition' (Mobbs 1968). In addition to this evidence of non-self-preserving development, the relative turbulent intensity is very large, the root-mean-square velocity fluctuation being more than the velocity defect (Kuo & Baldwin 1967). In appendix F, it is shown that, starting with measured values for the turbulent jet in still air, no real solution of the entrainment equation exists. If the condition of self-preserving development is relaxed, i.e. the ratio q_0/u_0 is allowed to vary, the similarity assumptions lead to the prediction that the ratio increases slowly but without limit, in agreement with the observations of very large turbulent intensities. It should be mentioned that the constants in the equation are completely different for axisymmetric wakes in 'tailored' pressure gradients (Newman 1968) and there self-preserving development is allowed.

A third example is the distorted wake studied by Reynolds (1962) and by Keffer (1965), which is a two-dimensional wake developing of constant area but lateral dimensions varying as e^{+ax} and e^{-ax}. The self-preserving flow exists if the plane of the wake is in the direction of expansion, and the analysis predicts that the width of the flow is proportional to $e^{-\frac{1}{2}ax}$. Keffer found that the width does not decrease appreciably and is roughly constant through the distorting duct. In appendix G, it is shown that no value of the entrainment rate is consistent with the similarity assumptions and self-preserving development, essentially because of the direct transfer of energy from the distortion flow to the turbulent motion. In all three examples, the inability to adopt a self-preserving configura-

tion leads to a greater proportion of the energy flux through any section of the flow being in the form of turbulent energy and an asymptotic approach to a condition with negligible variation of mean velocity within the flow.

8. The nature of the entrainment process

Applications of assumptions of structural similarity by Bradshaw *et al.* (1967), by Townsend (1966) and in the previous section show that it is possible to predict entrainment rates to within 10% for many free turbulent flows without needing to refer to the details of the entrainment process. On the other hand, the actual velocity with which ambient fluid passes through the turbulent 'front' is not a constant fraction either of the mean velocity variation or of the root-mean-square velocity fluctuation in the flow, and it appears that the effects of similarity dominate the control system determining the rate of entrainment. In that case, the actual entrainment process must adapt itself to produce the imposed rate of entrainment.

As it happens, details of entrainment have been studied in two flows with extreme values of the entrainment constant, two-dimensional wakes with very rapid entrainment and constant-pressure boundary layers with very slow entrainment. Expressed as fractions of the mean velocity variations, entrainment rates in the wake are about eight times as large as in the boundary layer, or about twice as large expressed as fractions of the root-mean-square velocity fluctuation. So it is not surprising that some prominent features of the entrainment process in wakes are not observed in boundary layers. In both flows, the interface between turbulent and non-turbulent fluid advances into the ambient fluid, probably by small-scale motions, but the rate of entrainment depends on continuous deformation and folding of the interface. Gartshore (1966) has shown that the amplitude of the folding is closely correlated with the entrainment rate, and it is likely that the small-scale erosion of the ambient fluid is really the final stage of the coarse entrainment by folding and engulfing by the large-scale motion of the interface.

The differences in the large-scale folding between wakes and boundary layers are marked. In wakes, Grant (1958) and Keffer (1965) have found that the surface distorts into short lengths of periodic waves with crests aligned across the flow and that they develop in a way that is very similar to the well-known instability of a vortex sheet. In agreement with the idea that the folding is caused by a Helmholtz type instability, the convection velocity of the folds is considerably different from that of the ambient fluid. In boundary layers, no tendency to periodic groups can be found and the convection velocity of the folds is hardly distinguishable from the ambient velocity (Kovasznay 1968). The differences in shape of the folding may be seen in the longitudinal and transverse correlation functions for $\delta(\mathbf{x}, t)$, the intermittency signal, and for η, the displacement of the interface from its mean position. For the wake, the longitudinal δ-correlation shows a distinct minimum and rather uncertain evidence of additional maxima and minima (figure 10). Multiple-correlation measurements also show a tendency to periodicity. The results in figures 11 and 12 are obtained from analysis of

ciné film taken by Fiedler & Head (1966) and show that, allowing for the effect of the small sample, both longitudinal correlations remain positive while the transverse correlations (in the $0x_2$ direction) take large negative values.

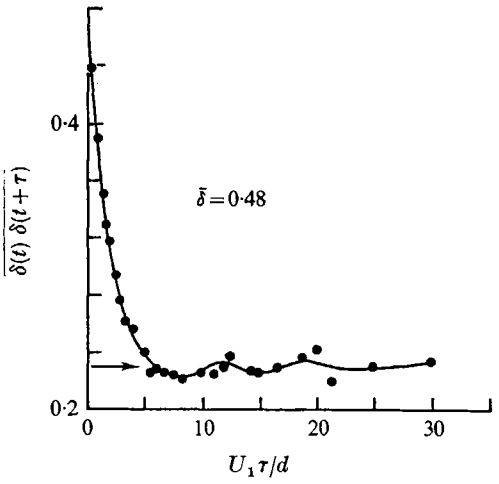

FIGURE 10. Time delay (effectively longitudinal) correlation function of an intermittency signal in a plane wake ($U_1 d/\nu$ = 6000, x/d = 150, intermittency factor of 0·48).

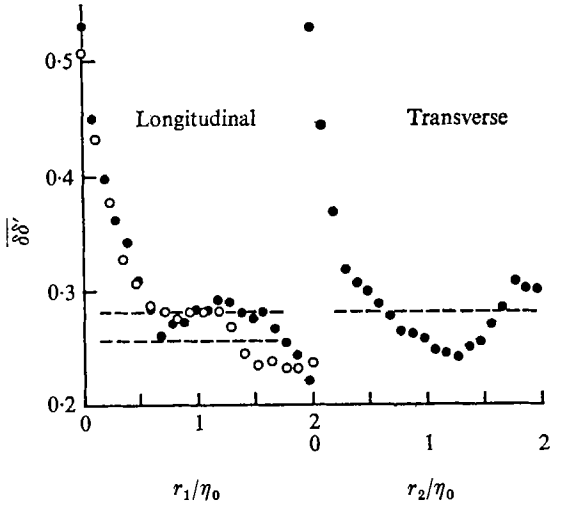

FIGURE 11. Longitudinal and transverse correlation functions of the intermittency signal in a constant-pressure boundary layer (from ciné film by Fiedler & Head (1966)).

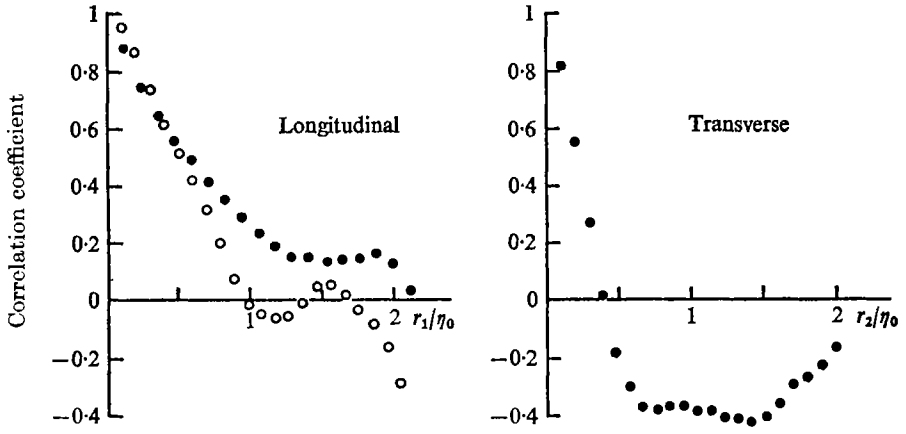

FIGURE 12. Longitudinal and transverse correlation coefficients for η, the displacement of the bounding surface, in a constant-pressure boundary layer (from ciné film by Fiedler & Head (1966)).

The nature of the interface folding in boundary layers indicates that it is the direct result of the velocity fields of the double-roller eddies of the main motion, which are typically outward movements along a longitudinal ridge flanked by inward flow on two parallel hollows. Folding of the interface that is driven by the

main turbulent motion may be regarded as the basic entrainment mechanism, and, if it exists in a pure form, it should, by dimensional argument, lead to a rate of entrainment that is proportional to the velocity scale of the turbulent motion. In the wake, other entrainment mechanisms operate but Grant finds that periods of active entrainment alternate with periods of quiescence during which entrainment is slow and probably is carried out by the basic mechanism. Supposing that only the basic entrainment occurs during the quiescent periods, fluid flows across the interface with an entrainment velocity,

$$w_0 = \beta_0 q_0, \tag{8.1}$$

where β_0 is a constant characteristic of the basic entrainment. Considering a small section of the interface and assuming longitudinal homogeneity, conservation of momentum requires that

$$w_0(U_1 - U) = \tau, \tag{8.2}$$

where τ is the Reynolds stress in the turbulent fluid (here treated as a continuum in which 'point' stresses and velocities are allowed). The close analogy between heat and Reynolds stress (Townsend 1956) suggests that stress increases rapidly with distance from the interface, and the equation indicates that velocity also increases sharply. As a fraction of the mean velocity scale u_0, the velocity jump is

$$\frac{U_1 - U}{u_0} = \frac{1}{\beta_0}\frac{\tau}{u_0 q_0} \propto \frac{1}{\beta_0}\frac{\tau^{\frac{1}{2}}}{q_0} R_s^{-\frac{1}{2}}, \tag{8.3}$$

and is expected to be more than twice as large in a wake ($R_s \approx 12$) as in a boundary layer ($R_s \approx 55$). If prolonged quiescence leads to an appreciable velocity jump, a Helmholtz instability of the interface is expected to develop and to cause additional active entrainment. If the velocity jump so calculated is small, the instability will be much weaker and its effects, and even its development, may be lost in the background of the basic entrainment.

To sum up, it is argued that the level of turbulent motion and the entrainment rate are set by the structure of the whole flow. The actual entrainment mechanism is a folding in and engulfing of the ambient fluid by movements of the interface which in general have two origins. The basic origin is the velocity fields of the eddies of the main turbulent motion but, particularly in flows with large entrainment rates, entrainment by the basic mechanism alone leads to an instability of the interface and to the initiation of a period of active, more rapid entrainment. The rapid entrainment destroys the velocity profile that caused the instability and the flow reverts to a quiescent condition with the basic entrainment rate. The differences in entrainment rates between flows are related to the relative durations of the active and quiescent periods and to the magnitude of the entrainment rate during the active periods.

The previous discussion of entrainment applies only to the 'main sequence' of free turbulent flows—wakes, jets, mixing layers and boundary layers—and it is not relevant to anomalous flows such as the axisymmetric, small-deficit wake or to flows with weak or negative entrainment rates—boundary layers in favourable pressure gradients and zero-momentum wakes. In these flows, the indentations of the interface are abnormally large (Fiedler & Head 1966; Mobbs

1968) but the net entrainment is small. Mobbs finds that the net entrainment in the zero-momentum wake is actually negative with some of the turbulent fluid reverting to (comparatively) non-turbulent motion, but that a positive net rate of entrainment is restored if the wake is distorted. In the anomalous flows, substantial turbulent intensities are found in regions of comparatively small rates of shear and it is likely that the deeply indented interface is indicative of shear-free inhomogeneous turbulence.

Appendix A. The effects on the space–time correlation function of eddy decay and movement

Use of the term 'eddy' rather than, say, 'Fourier component' implies that an adequate description of turbulent motion can be obtained by superimposing velocity distributions of the form

$$u_i(\mathbf{x}, t) = a(t) f_i(\mathbf{x} - \mathbf{x}_0(t)),$$

where $a(t)$ is the current amplitude of the eddy and $\mathbf{x}_0(t)$ is the position of its centre, and the eddy forms, defined by the functions f_i, depend mostly on a size parameter. Assuming that the energy-containing eddies can be described by eddies of a single kind, the space-time correlation function for homogeneous turbulence is

$$\begin{aligned} R_{ij}(\mathbf{r}, \tau; t) &= \langle u_i(\mathbf{x}, t)\, u_j(\mathbf{x}+\mathbf{r}, t+\tau)\rangle \\ &= n\left\langle a(t)\, a(t+\tau) \int f_i(\mathbf{x}-\mathbf{x}_0(t)) f_j(\mathbf{x}+\mathbf{r}-\mathbf{x}_0(t+\tau))\, dV(\mathbf{x}_0)\right\rangle, \end{aligned}$$

with the eddy centres occurring randomly in space with number density n. If the displacements of the eddy centres,

$$\Delta\mathbf{x}_0 = \mathbf{x}_0(t+\tau) - \mathbf{x}_0(t)$$

are independent of the changes in $a(t)$, the eddy amplitude, we have

$$\begin{aligned} R_{ij}(\mathbf{r}, \tau; t) &= n\langle a(t)\, a(t+\tau)\rangle \left\langle \int f_i(\mathbf{x}) f_j(\mathbf{x}+\mathbf{r}-\Delta\mathbf{x}_0)\, dV(\mathbf{x})\right\rangle \\ &= \frac{\langle a(t)\, a(t+\tau)\rangle}{\langle a^2(t)\rangle} \int R_{ij}(\mathbf{r}-\Delta\mathbf{x}_0, 0; t)\, P(\Delta\mathbf{x}_0)\, d(\Delta\mathbf{x}_0), \end{aligned}$$

where $P(\Delta\mathbf{x}_0)$ is the probability distribution function for a centre displacement $\Delta\mathbf{x}_0$ in the the time interval, t to $t+\tau$.

In this expression, the factor outside the integral depends on changes of eddy amplitude and its effect is to change the magnitude of the correlation function for fixed time-delay without affecting the form. The integral describes the effects of movement of eddies as a whole, either by their own velocity fields (as for vortex rings or Hill vortices) or by the velocity fields of other eddies, and its effect is equivalent to a diffusion of the function in correlation space. In other words, eddy movements reduce the magnitude of the correlation for small displacements but increase it for large ones, leading to larger spatial extent of the correlation function at fixed time delay.

Space-time correlations in the flow downstream of a biplane grid have been published by Favre *et al.* (1962) and by Frenkiel & Klebanoff (1967), and both show the increase in spatial extent. Assuming normal distribution of the centre displacements and isotropic turbulence with an exponential (spatial) correlation function (see equation (4.1)), the results of Favre *et al.* for a grid Reynolds number of 21,500 for $U_1\tau/M = 40$ can be fitted with $(\overline{\Delta x_0^2})^{\frac{1}{2}}/L = 0{\cdot}36$ and $\langle a(t)\,a(t+\tau)\rangle/[\langle a(t)^2\rangle\langle a(t+\tau)^2\rangle]^{\frac{1}{2}} = 0{\cdot}86$ for $U_1\tau/M = 7{\cdot}57$. The observed value of the correlation coefficient,

$$R_{11}(0_1\tau)/[\overline{u_1^2(t)\,u_1^2(t+\tau)}]^{\frac{1}{2}}$$

is 0·41, indicating that centre displacements are responsible for the greater part of the observed change in correlation in a frame of reference moving with the mean flow. Of the fall in the auto-correlation coefficient for the eddy amplitude from 1 to 0·86, a considerable part must be due to the natural growth in eddy size during decay rather than to changes of shape or basic structure.

From the magnitude of the inferred displacements, the root-mean-square velocity of the eddy centres can be estimated as $(\overline{\Delta x_0^2})^{\frac{1}{2}}/\tau$. It is interesting that it is within 10% of the root-mean-square velocity fluctuation, and it appears likely that the movement of the centres is a consequence of the eddy structure.

Appendix B. Calculation of intensities and correlation functions after rapid distortion by plane shearing

If a flow containing velocity fluctuations described by the Fourier coefficients of the series,

$$u_i = \sum_{\mathbf{k}} a_i(\mathbf{k}, t)\, e^{i\mathbf{k}.\mathbf{x}}$$

undergoes plane shearing by the mean flow,

$$U_1 = (d\alpha/dt)\, x_3, \quad U_2 = U_3 = 0,$$

neglect of the turbulent interaction terms in the equations of motion (Pearson 1959) leads to the result that the coefficients change so that

$$a_1(\mathbf{k}, t) = D\left[a_1(\mathbf{k}_0, 0) + \frac{k_0^2}{k_1^2+k_2^2}\left(-\frac{k_2^2}{k_0^2}P + \frac{k_1^2}{k_0^2}Q\right) a_3(\mathbf{k}_0, 0)\right],$$

$$a_2(\mathbf{k}, t) = D\left[a_2(\mathbf{k}_0, 0) + \frac{k_1 k_2}{k_1^2+k_2^2}\,(P+Q)\, a_3(\mathbf{k}_0, 0)\right],$$

$$a_3(\mathbf{k}, t) = D\,\frac{k_0^2}{k_0^2 - 2\alpha k_1 k_{30} + \alpha^2 k_1^2}\, a_3(\mathbf{k}_0, t),$$

$$\mathbf{k}_0 = \mathbf{k}(0) = (k_1, k_2, k_{30}),$$

$$\mathbf{k} = \mathbf{k}(t) = (k_1, k_2, k_{30} - \alpha k_1),$$

$$D = \exp\left[-\tfrac{1}{4}Nk_0^2L^2(1 - \alpha k_1 k_{30}/k_0^2 + \tfrac{1}{3}a^2k_1^2/k_0^2)\right],$$

$$P = \frac{k_0^2}{k_1(k_1^2+k_2^2)^{\frac{1}{2}}}\,\mathrm{artan}\left(\frac{\alpha k_1 (k_1^2+k_2^2)^{\frac{1}{2}}}{k_0^2 - \alpha k_1 k_{30}}\right),$$

$$Q = \alpha \frac{k_0^2 - 2k_{30}^2 + \alpha k_1 k_{30}}{k_0^2 - 2\alpha k_1 k_{30} + \alpha^2 k_1^2},$$

$$N = \frac{4\nu}{L^2 d\alpha/dt},$$

where α is the total strain, carried out at uniform rate. The changes are linear in the amplitudes and may be written as

$$a_i(\mathbf{k}, t) = DA_{ip} a_p(\mathbf{k}_0, 0),$$

where the tensor A_{ip} depends only on the direction of the wave-number vector and on α.

If the fluctuations are one realization of a field of homogeneous turbulence, the three-dimensional spectrum functions at the initial instant and at time t are related by

$$\Phi_{ij}(\mathbf{k}, t) = D^2 A_{ip} A_{jq} \Phi_{pq}(\mathbf{k}_0, 0)$$

or, if the initial turbulence is isotropic with the spectrum,

$$\Phi_{ij}(\mathbf{k}_0, 0) = (\delta_{ij} - k_i k_j / k_0^2)\, \psi(k_0)$$

by

$$\Phi_{ij}(\mathbf{k}, t) = D^2 [A_{ip} A_{jq} (\delta_{pq} - k_p k_q / k_0^2)]\, \psi(k_0).$$

Notice that the quantity inside the square brackets depends only on the direction of the wave-number vector and on α.

To calculate the changes of intensities and Reynolds stress, the appropriate spectrum function must be integrated over all wave-numbers, and, unless the viscous effects are negligible, the results depend on the spectral form, i.e. on the defining scalar $\psi(k_0)$. Since the purpose of including a viscous term is to model the effects of energy transfer to smaller eddies, it is appropriate to use a spectrum with a rapid cut-off at large wave-numbers, defined by

$$\psi(k_0) = (32\pi^3)^{-\frac{1}{2}} k_0^2 L^5 \exp(-\tfrac{1}{2} k_0^2 L_0^2).$$

In spherical polar co-ordinates for $\mathbf{k}_0$, integration with respect to k_0 can be done explicitly, and it is only necessary to compute the double integrals,

$$\overline{u_i u_j} = \int_0^{\pi} \int_0^{2\pi} \frac{3}{8\pi} [A_{ip} A_{jq} (\delta_{pq} - k_p k_q / k_0^2) \times (1 + N(1 - \alpha k_1 k_{30}/k_0^2 + \tfrac{1}{3}\alpha^2 k_1^2 / k_0^2))^{-\frac{5}{2}}] \sin\theta \, d\theta \, d\phi.$$

The quantity N measures the relative effect of energy loss from the large, energy-containing eddies of the turbulence compared with their gain from the shearing. With the error-law spectrum function, the rate of energy transfer is

$$\epsilon = 15\nu_e \overline{u_1^2}/L^2 = (\overline{q^2})^{\frac{3}{2}} L_\epsilon^{-1},$$

and so

$$N = \frac{4}{15} \frac{(\overline{q^2})^{\frac{3}{2}}}{\overline{u_1^2} L_\epsilon} \Big/ \frac{\partial U_1}{\partial x_3}.$$

In shear flows, typical values range from about 0·22 in wakes to about 0·08 in boundary layers. For the homogeneous shear flow of Rose (1966), the value is approximately 0·20.

The correlation functions were calculated for zero effective viscosity. Correlation functions for displacements in the direction of the unit vector $\hat{\mathbf{r}}$ can be approached through the one-dimensional spectrum function in that direction,

$$\phi_{ij}(l\hat{\mathbf{r}}) = 2\int\int \Phi_{ij}(\mathbf{k})\, dS(\mathbf{k}),$$

where $dS(\mathbf{k})$ is an element of the surface on which $\mathbf{k}.\hat{\mathbf{r}} = l$. Then

$$R_{ij}(r\hat{\mathbf{r}}) = \int_0^\infty \phi_{ij}(l\hat{\mathbf{r}}) \cos lr\, dl.$$

With spherical polar co-ordinates for $\mathbf{k}_0$,

$$\mathbf{k}_0 = lf\mathbf{n}.(\theta, \phi, \hat{\mathbf{r}})$$

on the surface of integration for $\phi_{ij}(l\hat{\mathbf{r}})$, and

$$R_{ij}(r\hat{\mathbf{r}}) = 2\int_0^\pi \int_0^{2\pi} A_{ip}A_{jq}(\delta_{pq} - k_p k_q/k_0^2)\left(\frac{\partial(k_a, k_b)}{\partial(\theta, \phi)}\right) l^{-2} \times \int_0^\infty l^2 \psi(k_0) \cos lr\, dl \sin\theta\, d\theta\, d\phi,$$

where k_a, k_b are orthogonal co-ordinates on the surface of integration. Then the integration over l leads to the Fourier transform of $l^2\psi(k_0)$. Choosing the defining scalar as

$$\psi(k_0) = \frac{2}{\pi^2}\overline{u_1^2}\frac{k_0^2 L^5}{(1+k^2L^2)^3}$$

(implying an initial correlation function of exponential form,

$$R_{11}(r, 0, 0) = \overline{u_1^2} e^{-r/L}),$$

$$\int_0^\infty l^2 \psi(k_0) \cos lr\, dl = \frac{1}{4\pi}\left(\frac{l}{k_0}\right)^3 \left(3 - 5\frac{lr}{k_0 L} + \left(\frac{lr}{k_0 L}\right)^2\right) \exp\left(-\frac{lr}{k_0 L}\right)$$

and the computation of the correlation functions reduces to evaluation of a double integral over the angle variables.

Appendix C. Distributions of effective strain in self-preserving flows

In a plane wake with small velocity defect and no pressure gradient, the equations for the distribution functions of velocity and effective strain, (5.3) and (5.4), become

$$-\frac{U_1 l_0}{\nu_T}\frac{dl_0}{dx}\eta f = f'$$

and

$$-\frac{U_1}{u_0}\frac{dl_0}{dx}\left(\frac{D_T}{\nu_T}k'' + \eta k'\right) = f'.$$

If the length scale is defined so that

$$\frac{U_1 l_0}{\nu_T}\frac{dl_0}{dx} = 1$$

the solutions are $$f(\eta) = \exp(-\tfrac{1}{2}\eta^2)$$

and, for the special but relevant case of $\nu_T = D_T$,

$$k(\eta) = -\tfrac{1}{2}R_s\eta\exp(-\tfrac{1}{2}\eta^2) + C\int_0^\eta \exp(-\tfrac{1}{2}x^2)\,dx,$$

where $R_s = u_0 l_0/\nu_T$ is the flow constant. The constant of integration C should be chosen to make the effective strain small at the mean position of entrainment, which is nearly at $\eta = 2$. Then

$$k(\eta) = -\tfrac{1}{2}R_s\left[\eta\exp(-\tfrac{1}{2}\eta^2) - 0{\cdot}226\int_0^\eta \exp(-\tfrac{1}{2}x^2)\,dx\right]$$

and the maximum value occurs near $\eta = 1$ and is nearly $0{\cdot}21R_s$ or $2{\cdot}6$.

For a plane jet issuing into still fluid, the equations for the distribution functions may be put into the forms,

$$-\frac{1}{2}\frac{dl_0}{dx}\frac{u_0 l_0}{\nu_T}\left(f^2 + f'\int_0 f\,d\eta\right) = f''$$

and

$$-\frac{1}{2}\frac{dl_0}{dx}\frac{u_0 l_0}{D_T}\left(k'\int_0 f\,d\eta\right) + k'' = f'\frac{u_0 l_0}{D_T}.$$

If the length scale is defined so that

$$\frac{1}{4}\frac{u_0 l_0}{\nu_T}\frac{dl_0}{dx} = 1,$$

the solutions are $$f(\eta) = \operatorname{sech}^2\eta$$

and, for $\nu_T = D_T$,

$$k(\eta) = 2{\cdot}71R_s(\tanh\eta\log(\cosh\eta) - \eta + C\tanh\eta).$$

The factor $2{\cdot}71$ appears because R_s is defined with the distance between the jet centre and the position where $U/u_0 = f(\eta) = e^{-\frac{1}{2}}$, in this case at $\eta = 0{\cdot}738$. Choosing C as $0{\cdot}803$ makes the effective strain zero at twice this distance (compare the wake calculation), and the maximum value of the effective strain occurs near $\eta = 0{\cdot}74$ and is nearly $0{\cdot}22R_s$ or $6{\cdot}1$.

For a mixing layer between streams of nearly equal velocity, the equations become

$$-\frac{U_1 l_0}{\nu_T}\frac{dl_0}{dx}\eta f' = f''$$

and

$$-\frac{U_1 l_0}{D_T}\frac{dl_0}{dx}\eta k' - k'' = f'\frac{u_0 l_0}{D_T}.$$

Defining the length-scale so that

$$\frac{U_1 l_0}{\nu_T}\frac{dl_0}{dx} = 1,$$

the solutions are $$f(\eta) = (2\pi)^{-\frac{1}{2}}\int_{-\infty}^{\eta} \exp(-\tfrac{1}{2}x^2)\,dx$$

and for $\nu_T = D_T$, $$k(\eta) = \frac{R_s}{(2\pi)^{\frac{1}{2}}}[\exp(-\tfrac{1}{2}\eta^2) - C].$$

Without measurements of intermittency in the plane mixing layer, it is necessary to guess the mean positions of the bounding surface, it is not likely to be very far from the position $\eta = \pm 1{\cdot}4$, where the mean velocity is within 5% of the stream velocity on that side. Then the constant C is 0·37 and the maximum effective strain, at the flow centre, is $0{\cdot}25R_s$ or about 7·5.

The calculation for a boundary layer is similar to that for mixing layers, the differences arising from the absence of symmetry and uncertainty as to the effective strain in the constant-stress layer. The range of values in table 3 refers to possible values of this effective strain in the range 5–15.

Appendix D. Entrainment constants for mixing layers between parallel streams

Consider a mixing layer between streams of velocities U_1 and $U_2 = U_1 + u_0$ with the self-preserving distribution of mean velocity,

$$U = U_1 + u_0 f(z/l_0).$$

The momentum equation is

$$-\frac{dl_0}{dx}\left[\frac{U_1}{u_0}\eta f' + f'\int_0 f\,d\eta\right] + g'_{12} = 0$$

if the axes are chosen so that $W = 0$ along the plane $z = 0$. Notice that this plane is also the plane of maximum shear-stress. Integration of the equation across the flow leads to the momentum condition,

$$(I_1 - I_2)\frac{U_1}{u_0} + I_{12} - I_2 + I_{22} = 0,$$

where

$$I_1 = \int_{-\infty}^{0} f\,d\eta, \quad I_2 = \int_0^{\infty} (1-f)\,d\eta,$$

$$I_{12} = \int_{-\infty}^{0} f^2\,d\eta, \quad I_{22} = \int_0^{\infty} (1-f)^2\,d\eta,$$

$$I_a = \int_{-\infty}^{\infty} \eta f^2 f'\,d\eta, \quad I_b = \int_{-\infty}^{\infty} \eta f f'\,d\eta,$$

are non-dimensional integrals of the distribution function. Integration of the momentum equation from one free stream to the centre leads to

$$-g(0) = \frac{\tau_m}{u_0^2} = \frac{dl_0}{dx}\left[\frac{U_1}{u_0}I_1 + I_{12}\right].$$

The equation for conservation of total energy (mean flow and fluctuation kinetic energy) is

$$\frac{1}{2}\int_{-\infty}^{\infty} \frac{\partial}{\partial x}[U(\overline{(U-U_1)^2} + \overline{q^2})]\,dz + \tfrac{1}{2}W_2(U_2 - U_1)^2 = -\int_{-\infty}^{\infty} \epsilon\,dz,$$

where $$W_2 = -\int_0^\infty (\partial U/\partial x)\, dz$$

is the normal velocity in the far stream. After substitution of the similarity profiles and use of the relation between τ_m/u_0^2 and the rate of spread, the energy equation becomes

$$\frac{U_1}{u_0} I_b + \tfrac{3}{2} I_a - \tfrac{1}{2} I_2 - \frac{1}{2}\frac{q_0^2}{\tau_m}\frac{dl_0}{dx}\left[\frac{U_1}{u_0} I_1 + I_{12}\right]\left[\frac{U_1}{u_0}(\eta_2 - \eta_1) + \int_{\eta_1}^{\eta_2} f\, d\eta\right]$$
$$= \frac{l_0}{L_\epsilon}(\eta_2 - \eta_1)\left[\frac{U_1}{u_0} I_1 + I_{12}\right]^{\frac{3}{2}}\left(\frac{q_0^2}{\tau_m}\right)^{\frac{3}{2}}\left(\frac{dl_0}{dx}\right)^{\frac{1}{2}},$$

where q_0^2 is chosen so that it is an average value of $\overline{q^2}$ within the bounding surfaces, i.e.

$$\int_{-\infty}^{\infty} \overline{q^2}\, dz = (\eta_2 - \eta_1)\, q_0^2\, l_0$$

and L_ϵ is chosen so that $$\int_{-\infty}^{\infty} \epsilon\, dz = (\eta_2 - \eta_1)\, q_0^3\, l_0/L_\epsilon,$$

η_1 and η_2 defining the average positions of the two bounding surfaces. Approximating the velocity profiles by the error integral,

$$f(\eta) = \frac{1}{(2\pi)^{\frac{1}{2}}}\int_{-\infty}^{\eta+\eta_0} \exp(-\tfrac{1}{2}x^2)\, dx,$$

substitution in the overall momentum condition shows that

$$\eta_0 = \frac{2^{\frac{1}{2}} - 1}{(2\pi)^{\frac{1}{2}}}\left(\frac{U_1}{u_0} + \frac{1}{2}\right)^{-1},$$

if η_0 is not too large. The non-dimensional integrals are

$$I_1 = (2\pi)^{-\frac{1}{2}} + \tfrac{1}{2}\eta_0, \quad I_2 = (2\pi)^{-\frac{1}{2}} - \tfrac{1}{2}\eta_0,$$

$$I_{12} = \frac{2^{\frac{1}{2}} - 1}{2\pi^{\frac{1}{2}}} + \tfrac{1}{4}\eta_0, \quad I_{22} = \frac{2^{\frac{1}{2}} - 1}{2\pi^{\frac{1}{2}}} - \tfrac{1}{4}\eta_0,$$

$$I_a = \frac{1}{2\pi^{\frac{1}{2}}} - \tfrac{1}{3}\eta_0, \quad I_b = \frac{1}{2\pi^{\frac{1}{2}}} - \tfrac{1}{2}\eta_0,$$

and the energy equation is now

$$2^{-\frac{1}{2}} - \frac{1}{2}\frac{q_0^2}{\tau_m}\frac{dl_0}{dx}\left[\frac{U_1}{u_0}(\eta_2 - \eta_1) + \int_{\eta_1}^{\eta_2} f\, d\eta\right] = (2\pi)^{-\frac{1}{4}}(\eta_2 - \eta_1)\frac{l_0}{L_\epsilon}\left(\frac{U_1}{u_0} + \frac{1}{2}\right)^{\frac{1}{2}}\left(\frac{q_0^2}{\tau_m}\right)^{\frac{3}{2}}\left(\frac{dl_0}{dx}\right)^{\frac{1}{2}}.$$

From the measurements of Watt (1967), it may be estimated that $\eta_1 = -1{\cdot}0$, $\eta_2 = 1{\cdot}4$, and so, very nearly,

$$\int_{\eta_1}^{\eta_2} f\, d\eta = \tfrac{1}{2}(\eta_2 - \eta_1).$$

In that case, the entrainment constant,

$$\beta = \left(\frac{U_1}{u_0} + \frac{1}{2}\right)\frac{dl_0}{dx}$$

is given by the equation

$$2^{-\frac{1}{2}} - \tfrac{1}{2}(\eta_2 - \eta_1)\frac{q_0^2}{\tau_m}\beta = (2\pi)^{-\frac{1}{4}}(\eta_2 - \eta_1)\frac{l_0}{L_\epsilon}\left(\frac{q_0^2}{\tau_m}\right)^{\frac{3}{2}}\beta^{\frac{1}{2}}$$

and the velocity ratio does not appear explicitly.

The equation for effective strain is for $\eta = 0$

$$0 = (2\pi)^{-\frac{1}{2}}\frac{u_0}{l_0} + D_T l_0^{-2}\left(\frac{\partial^2 \alpha}{\partial \eta^2}\right)_{\eta=0}$$

and, assuming similarity of the profiles of effective strain, the maximum value is

$$\alpha_m = c'\frac{u_0 l_0}{D_T} = cR_s.$$

The previous relation between τ_m/u_0^2 and dl_0/dx is, for the assumed profile,

$$\frac{\tau_m}{u_0^2} = (2\pi)^{-\frac{1}{2}}\beta = (2\pi)^{-\frac{1}{2}}R_s$$

and so α_m is proportional to β. If the effective value of q_0^2/τ_m is determined by the effective strain, the equation for the entrainment constant shows that it should be nearly independent of the velocity ratio of the two streams.

Appendix E. The effect of wall curvature on the spread of a wall jet

In a wall jet, the velocity maximum occurs at a comparatively small distance from the solid boundary and the flow between the velocity maximum and the free stream resembles closely one half of a plane jet. The only important difference arises from the mean flow across the plane of maximum stress which is a consequence of the wall friction. If the wall layer between the wall and the plane of maximum velocity is thin, consideration of the momentum balance shows that

$$-U_m W_m = \tau_0 - (\tau_m)$$

(suffix m denotes value at the plane) and (τ_m) is expected to be small at a place of zero velocity gradient.

Self-preserving flow of a wall jet over a curved surface is dynamically possible if (i) the radius of curvature of the surface is everywhere the same fraction of the jet thickness, and (ii) the ratio of friction velocity to the maximum velocity remains constant. The last condition is satisfied approximately if the Reynolds number of the flow is large. With no external flow, the flow thickness is proportional to distance from a virtual origin and the maximum velocity varies inversely as the square-root of distance from the origin.

Consider the flow in cylindrical polar co-ordinates with axis coinciding locally with the axis of curvature of the surface. The equation for the mean velocity is

$$\frac{\partial U^2}{\partial \theta} + \frac{\partial (UWr)}{\partial r} + \frac{\partial (\overline{uwr})}{\partial r} = -\frac{\partial P}{\partial \theta}$$

to the usual boundary-layer approximation. Integrating from $z = z_m$ at the

velocity maximum to the ambient flow gives

$$\frac{\partial}{\partial\theta}\int_{R+z_m}^{\infty} U^2\,dr = -\frac{\partial}{\partial\theta}\int_{R+z_m}^{\infty} P\,dr - \tau_0 R.$$

To the same approximation, the equation for the velocity normal to the surface is

$$\frac{\partial P}{\partial r} = \frac{U^2}{r},$$

and so

$$P = -\int^{\infty} \frac{U^2}{r}\,dr$$

and

$$\int_{R+z_m}^{\infty} P\,dr = R\int_{R+z_m}^{\infty} \frac{U^2}{r}\,dr - \int_{R+z_m}^{\infty} U^2\,dr.$$

It follows that

$$\frac{d}{d\theta}\left[R\int_{R+z_m}^{\infty} \frac{U^2}{r}\,dr\right] = -\tau_0 R,$$

or, if $(r-R) \ll R$,

$$\frac{d}{d\theta}\int_{z_m}^{\infty} U^2(1-z/R)\,dz = -\tau_0 R,$$

where $z = (r-R)$.

The equation for the kinetic energy of the flow is

$$\frac{d}{d\theta}\int_{z_m}^{\infty} [\tfrac{1}{2}U(U^2+\overline{q^2}) + PU]\,dz = -\tau_0 U_m R - \int_{z_m}^{\infty} \epsilon(R+z)\,dz$$

and, making the assumptions of profile similarity, we find that

$$\frac{d}{d\theta}\left[u_0^2 l_0\left(I_2 - \frac{l_0}{R} I_{2a}\right)\right] = -c_f u_0^2 R$$

and

$$\frac{d}{d\theta}\left[u_0^3 l_0\left(\tfrac{1}{2}I_3 + I_p\frac{l_0}{R}\right) + \tfrac{1}{2}q_0^2 u_0 l_0 I_1\right] = -c_f u_0^3 - q_0^3\frac{\eta_0}{L_\epsilon}\left(1+\frac{1}{2}\frac{\eta_0}{R}\right),$$

where $c_f = \tau_0/u_0^2$,

$$I_n = \int_0^{\infty} [f(x)]^n\,dx, \quad I_{2a} = \int_0^{\infty} [f(x)]^2\,x\,dx, \quad I_p = -\int_0^{\infty} f(x)\int_x^{\infty} [f(y)]^2\,dy\,dx.$$

For convenience, the non-dimensional co-ordinate is taken to be $\eta = (z-z_m)/l_0$. The system of equations is completed by a relation between the angle of spread and the ratio τ_m/u_0^2, and by the relation between effective strain and the value of q_0^2/τ_m. At $z = z_m$, the equation of motion is nearly

$$\frac{\partial(\tau r)}{\partial z} = \frac{1}{R}\frac{\partial}{\partial\theta}(P + \tfrac{1}{2}U^2)$$

and, since

$$P(z_m) = -\frac{l_0}{R} I_2 u_0^2,$$

$$\left(\frac{\partial(\tau r)}{\partial z}\right)_{z=z_m} = \frac{1}{R}\frac{\partial}{\partial\theta}\left[\tfrac{1}{2}u_0^2\left(1 - 2I_2\frac{l_0}{R}\right)\right].$$

Assuming similarity of the stress profiles, the maximum stress is

$$\tau_m = -c_1(1-l_0/R)\,(1-2I_2 l_0/R)\,\frac{l_0}{R}\frac{d}{d\theta}(u_0^2).$$

The discussion of the effect of wall curvature can be simplified by ignoring the wall stress, which is justified if both curvature and wall stress act as perturbations of the basic plane jet. Otherwise, the known behaviour of the plane jet must be used to determine the various parameters, such as η_0/l_0, L_ϵ/l_0 and τ_m/q_0^2. In the absence of wall stress,

$$u_0^2 l_0\left(I_2 - I_{2a}\frac{l_0}{R}\right) = M$$

a constant, and from the known variation of the scales in self-preserving flow, the energy equation becomes

$$\frac{1}{4}\left(I_3 + 2I_p\frac{l_0}{R} + \frac{q_0^2}{u_0^2}I_1\right) = \frac{q_0^3}{u_0^3}\frac{\eta_0}{L_\epsilon}\left(1+\frac{1}{2}\frac{\eta_0}{R}\right)\left(\frac{1}{R}\frac{dl_0}{d\theta}\right)^{\frac{1}{2}}.$$

Inserting the ratio τ_m/u_0^2, and defining

$$\beta = \frac{1}{R}\frac{dl_0}{d\theta}$$

the equation becomes

$$\left(I_3 + 2I_p\frac{l_0}{R}\right) + C_1\frac{q_0^2}{\tau_m}\left(1-(1+2I_2)\frac{l_0}{R}\right)\beta$$

$$= 2\left(C_1\frac{q_0^2}{\tau_m}\right)^{\frac{3}{2}}\frac{\eta_0}{L_\epsilon}\left[1+\left(\frac{1}{2}\frac{\eta_0}{l_0} - 3I_2 - \frac{3}{2}\right)\frac{l_0}{R}\right]\beta^{\frac{1}{2}},$$

where C_1 is a constant. As usual, the ratio q_0^2/τ_m is a function of effective strain or τ_m/u_0^2. For moderate values of l_0/R, the solution can be found by iteration and is

$$\beta = \beta_0\left[1+\frac{l_0}{R}\left(\frac{6I_2+3-\eta_0/l_0+4I_p/I_3-Q(1+2I_2+2I_p/I_2)}{1-2Q}\right)\right],$$

where β_0 is the value for zero curvature, and Q is the ratio of the advective gain of turbulent energy to the energy dissipation. For a profile shape,

$$f(\eta) = \exp(-\tfrac{1}{2}\eta^2),$$

$$I_2 = \tfrac{1}{2}\pi^{\frac{1}{2}}, \quad I_3 = \pi^{\frac{1}{2}}/6^{\frac{1}{2}}, \quad I_p = 0{\cdot}50,$$

and $\eta_0/l_0 \approx 2{\cdot}0$. Measurements of a plane jet (Bradbury 1965) suggest that $Q \approx 0{\cdot}15$, and then

$$\beta = \beta_0(1+4{\cdot}8l_0/R).$$

No allowance has been made for a variation of τ_m/q_0^2. For $\tau_m/q_0^2 \propto \beta^{-\frac{1}{3}}$, the coefficient of l_0/R is about 2·0, but the calculated effect of curvature is still comparable with that observed.

Appendix F. Conditions for self-preserving development in axisymmetric wakes and jets

Consider first the axisymmetric jet. If self-preserving development occurs, the equations for momentum and energy show that

$$u_0^2 l_0^2 = \text{constant}, \quad \frac{dl_0}{dx} = \beta = \text{constant}.$$

The equation for the total kinetic energy is

$$\frac{d}{dx}\frac{1}{2}\int_0^\infty U(U^2+\overline{q^2})\,r\,dr = -\int_0^\infty \epsilon\, r\,dr$$

or, after substituting the self-preserving forms,

$$\beta u_0^3 l_0 \left(I_3 + \frac{q_0^2}{u_0^2} I_1\right) = \frac{q_0^3}{L_\epsilon}\eta_0^2,$$

where

$$I_n = \int_0^\infty [f(x)]^n\, x\,dx.$$

To estimate the maximum shear stress, we know that, on the axis,

$$\frac{1}{r}\frac{\partial(\tau r)}{\partial r} = u_0\frac{du_0}{dx} = -\frac{u_0^2}{l_0}\frac{dl_0}{dx},$$

i.e.

$$\frac{\partial \tau}{\partial r} = -\tfrac{1}{2}\beta\, u_0^2/l_0$$

and, approximately,

$$\tau_m = \tfrac{1}{2}C_1\beta u_0^2,$$

where C_1 is a constant about $e^{-\frac{1}{2}}$ or 0·6. Then the energy equation becomes

$$I_3 + \tfrac{1}{2}C_1\frac{q_0^2}{\tau_m}I_1\beta = \frac{1}{2\sqrt{2}}\left(C_1\frac{q_0^2}{\tau_m}\right)^{\frac{3}{2}}\frac{\eta_0^2}{l_0 L_\epsilon}\beta^{\frac{1}{2}}$$

and has a real root if

$$C_1\frac{q_0^2}{\tau_m}\frac{\eta_0^2}{l_0 L_\epsilon}(I_1 I_3)^{-\frac{1}{2}} > 4.$$

The development of a self-preserving, axisymmetric wake with small velocity defect is described by

$$U_1 u_0 l_0^2 = \text{constant}, \quad \frac{U_1}{u_0}\frac{dl_0}{dx} = \beta = \text{constant},$$

and the equation for the total energy is

$$\tfrac{1}{2}U_1\frac{d}{dx}\int_0^\infty [(U-U_1)^2+\overline{q^2}]\,r\,dr = -\int_0^\infty \epsilon r\,dr.$$

Substitution of the similar profiles leads to

$$2\beta u_0^3 l_0\left[I_2 + \frac{1}{2}\frac{q_0^2}{u_0^2}\frac{\eta_0^2}{l_0^2}\right] = \frac{q_0^3}{L_\epsilon}\eta_0^2.$$

On the axis, $$\frac{1}{r}\frac{\partial(\tau r)}{dr} = U_1\frac{du_0}{dx} = -2\beta u_0^2/l_0$$

and $$\frac{\partial\tau}{\partial r} = -\beta u_0^2/l_0.$$

Then, as before $$\tau_m = C_1 u_0^2\beta,$$

and the equation for the entrainment constant is

$$I_2 + \tfrac{1}{2}C_1\frac{q_0^2}{\tau_m}\frac{\eta_0^2}{l_0^2}\beta = \frac{1}{2}\left(C_1\frac{q_0^2}{\tau_m}\right)^{\frac{3}{2}}\frac{\eta_0^2}{l_0 L_\epsilon}\beta^{\frac{1}{2}}.$$

It has real roots if $$2^{\frac{1}{2}}C_1\frac{q_0^2}{\tau_m}\frac{\eta_0}{L_\epsilon}(I_2)^{-\frac{1}{2}} > 4.$$

Approximating the velocity distribution by

$$f(\eta) = e^{-\frac{1}{2}\eta^2}$$

the constants are $$I_1 = 1, \quad I_2 = \tfrac{1}{2}, \quad I_3 = \tfrac{1}{3},$$

and measurements in jets show that, nearly,

$$\eta_0/l_0 = 2, \quad L_\epsilon/\eta_0 = 1{\cdot}5.$$

With these values, the jet may develop in a self-preserving way if

$$C_1 q_0^2/\tau_m > 1{\cdot}73,$$

and a wake may if $$C_1 q_0^2/\tau_m > 3{\cdot}0.$$

With the current approximations to the profiles, the ratio of total turbulent energy to total mean flow energy in a jet is

$$\int_0^\infty \overline{q^2}\, r\, dr \Big/ \int_0^\infty (U - U_1)^2 r\, dr = C_1\frac{q_0^2}{\tau_m}\frac{1}{4}\frac{\eta_0^2}{l_0^2}\frac{\beta}{I_2},$$

and measurements in jets indicate that it is near 0·4. Inserting the observed rate of spread of a jet, $\beta = 0{\cdot}08$, we find that

$$C_1 q_0^2/\tau_m = 2{\cdot}5,$$

sufficient for self-preserving development of a jet but not for a wake. If account is taken of the likely variation of q_0^2/τ_m with entrainment constant, the value of $C_1 q_0^2/\tau_m$ for a wake is less than that for a jet and the inequality is worse.

Appendix G. The condition for self-preserving flow of a distorted wake

Consider a plane wake immersed in the ambient flow,

$$U_1 = \text{constant}, \quad V_1 = \alpha U_1 y, \quad W_1 = -\alpha U_1 z.$$

The equation for the momentum flow is

$$U_1\frac{d}{dx}\int_0^\infty (U - U_1)\, dz + \alpha U_1\int_0^\infty (U - U_1)\, dz = 0$$

and self-preserving development is consistent with the momentum and energy equation if

$$u_0 \propto l_0 \propto e^{-\frac{1}{2}\alpha x}.$$

The equation for the total energy is

$$\tfrac{1}{2}U_1 \frac{d}{dx}\int_0^\infty [(U-U_1)^2+\overline{q^2}]\,dz + \tfrac{1}{2}\alpha U_1 \int_0^\infty [(U-U_1)^2+\overline{q^2}]\,dz + \alpha U_1 \int_0^\infty (\overline{u^2}-\overline{w^2})\,dz = -\int_0^\infty \epsilon\,dz$$

including a term $\alpha U_1 \int_0^\infty (\overline{v^2}-\overline{w^2})\,dz$ describing the generation of turbulent energy by working of the ambient velocity field against normal Reynolds stresses induced by the distortion. In terms of the similarity functions, the energy equation is

$$\tfrac{1}{4}\beta\left(I_2+\frac{q_0^2}{u_0^2}\frac{\eta_0}{l_0}+4\frac{q_0^2}{u_0^2}I_{23}\right)=\frac{\eta_0}{L_\epsilon}\frac{q_0^3}{u_0^3},$$

where

$$I_2=\int_0^\infty (f(x))^2\,dx$$

and

$$I_{23}=-q_0^{-2}l_0^{-1}\int_0^\infty (\overline{u^2}-\overline{w^2})\,dz.$$

The entrainment constant is $\beta = \alpha U_1 l_0/u_0$.

At the central plane of the wake,

$$\frac{\partial \tau}{\partial z}=U_1\frac{du_0}{dx}=-\tfrac{1}{2}\alpha U_1 u_0$$

and so

$$\tau_m=\tfrac{1}{2}C_1 u_0^2\beta.$$

Then the equation for the entrainment constant becomes

$$2I_2+C_1\frac{q_0^2}{\tau_m}\left(\frac{\eta_0}{l_0}+4I_{23}\right)\beta = 2^{\frac{3}{2}}\left(C_1\frac{q_0^2}{\tau_m}\right)^{\frac{3}{2}}\frac{\eta_0}{L_\epsilon}\beta^{\frac{1}{2}},$$

with real roots if

$$I_2(\eta_0/l_0+4I_{23}) < \frac{\eta_0^2}{L_\epsilon^2}\left(C_1\frac{q_0^2}{\tau_m}\right)^2.$$

After a total strain of about three, the ratio $(\overline{v^2}-\overline{w^2})/(\overline{v^2}+\overline{w^2})$ is about $-0{\cdot}4$ and the integral I_{23} is about $1{\cdot}0$. Substituting values of the constants for the plane wake, real roots are expected if

$$2+4I_{23} < 0{\cdot}50(C_1 q_0^2/\tau_m)^2,$$

a condition that cannot be satisfied for any plausible values of $C_1 q_0^2/\tau_m$ and of I_{23}. The implication is that the proportion of turbulent energy derived from interaction between the turbulent motion and the distortion becomes large compared with that derived from the mean flow energy of the wake proper.

REFERENCES

BALDWIN, L. V. & SANDBORN, V. A. 1968 *A.I.A.A. J.* **6**, 1163.

BATCHELOR, G. K. & PROUDMAN, I. 1954 *Quart. J. Mech. appl. Math.* **7**, 83.

BOWDEN, K. F. & HOWE, M. R. 1963 *J. Fluid Mech.* **17**, 271.

BRADBURY, L. J. S. 1965 *J. Fluid Mech.* **23**, 31.

BRADSHAW, P., FERRISS, D. H. & ATWELL, N. P. 1967 *J. Fluid Mech.* **28**, 593.

BRADSHAW, P., FERRISS, D. H. & JOHNSON, R. F. 1964 *J. Fluid Mech.* **19**, 591.

COMTE-BELLOT, G. 1961 *C. r. hebd. Séanc. Acad. Sci., Paris*, **253**, 2846.

COMTE-BELLOT, G. & CORRSIN, S. 1966 *J. Fluid Mech.* **25**, 657.

FAVRE, A., GAVIGILO, J. & DUMAS, R. 1957 *J. Fluid Mech.* **2**, 313.

FAVRE, A., GAVIGLIO, J. & DUMAS, R. 1962 *La Mécanique de la Turbulence*, p. 419. Paris: C.N.R.S.

FEKETE, G. I. 1963 *Mech. Eng. Dept., McGill Univ., Montreal, Report* 63–11.

FIEDLER, H. & HEAD, N. R. 1966 *J. Fluid Mech.* **25**, 719.

FRENKIEL, P. N. & KLEBANOFF, P. S. 1967 *Phys. Fluids*, **10**, 1737.

GARTSHORE, I. S. 1966 *J. Fluid Mech.* **24**, 89.

GIBSON, C. H., LIN, S. C. & CHEN, C. C. 1967 *A.I.A.A. J.* **6**, 642.

GRANT, H. L. 1958 *J. Fluid Mech.* **4**, 149.

KEFFER, J. F. 1965 *J. Fluid Mech.* **22**, 135.

KLINE, S. J., REYNOLDS, W. C., SCHRAUB, F. A. & RUNSTADLER, P. W. 1967 *J. Fluid Mech.* **30**, 741.

KOVASZNAY, L. S. G. 1968 *NATO Symposium on Transition*. London.

KUO, Y.-H. & BALDWIN, L. V. 1967 *J. Fluid Mech.* **27**, 353.

LUMLEY, J. L. 1965 Atmospheric turbulence and radio wave propagation. *Proc. Intern. Colloquium, Moscow.*

MARÉCHAL, J. 1967 *C. r. hebd. Séanc. Acad. Sci., Paris*, **265**A, 478.

MOBBS, F. R. 1968 *J. Fluid Mech.* **33**, 227.

NEE, V. W. & KOVASZNAY, L. S. G. 1969 *Phys. Fluids*, **12**, 473.

NEWMAN, B. G. 1968 *Mech. Eng. Dept., McGill Univ., Montreal, Report* 68–10.

PAYNE, F. R. 1966 *Dept. Aerospace Eng., Penn. State Univ.*

PEARSON, J. R. A. 1959 *J. Fluid Mech.* **5**, 274.

REYNOLDS, A. J. 1962 *J. Fluid Mech.* **13**, 333.

ROSE, W. G. 1966 *J. Fluid Mech.* **25**, 97.

SABIN, C. M. 1963 *Stanford Univ. Report* MD-9.

STEWART, R. W. 1951 Ph.D. Dissertation, University of Cambridge.

TRITTON, D. J. 1967 *J. Fluid Mech.* **28**, 439.

TOWNSEND, A. A. 1954 *Quart. J. Mech. appl. Math.* **4**, 308.

TOWNSEND, A. A. 1956 *The Structure of Turbulent Shear Flow*. Cambridge University Press.

TOWNSEND, A. A. 1966 *J. Fluid Mech.* **26**, 689.

TUCKER, H. J. & REYNOLDS, A. J. 1968 *J. Fluid Mech.* **32**, 1968.

WATT, W. E. 1967 *Dept. Mech. Eng., Univ. of Toronto*, TP 6705.